

ORIGINAL ARTICLE

# Healing Mechanism Surrounding Transplanted Bone Using Transgenic Mice Expressing Red Fluorescent Protein *in Vivo*

Manabu INOUE<sup>1</sup>, Keishi OTSU<sup>2</sup>, Masato OHTSUKA<sup>3</sup>,  
Kyoko TAKAFUJI<sup>1</sup>, Hidemitsu HARADA<sup>2</sup>,  
Akira ISHISAKI<sup>4</sup>, and Hisatomo KONDO<sup>1</sup>

<sup>1</sup> Department of Prosthodontics and Oral Implantology,  
School of Dentistry, Iwate Medical University, Morioka, Japan

<sup>2</sup> Division of Developmental Biology & Regenerative Medicine,  
Department of Anatomy,  
Iwate Medical University, Morioka, Japan

<sup>3</sup> Department of Molecular Life Science,  
Division of Basic Medical Science and Molecular Medicine,  
Tokai University School of Medicine, Kanagawa, Japan

<sup>4</sup> Division of Cellular Biosignal Sciences, Department of Biochemistry,  
Iwate Medical University, Morioka, Japan

## SYNOPSIS

In recent years, Use of dental implants is becoming more widespread; however, not all patients can receive implant treatment without bone grafting. Bone grafting is frequently performed in implant treatments, and graft materials include autogenous bone, allografts, xenografts, and alloplasts. The healing mechanism of the autogenous bone graft is not well known; therefore, this study examines the healing mechanism surrounding grafted bone, at both cellular and molecular levels, employing tissue derived from transgenic mice expressing red fluorescent protein *in vivo* to monitor cellular kinetics *in situ* and to elucidate the healing mechanism. Results of our study suggested that mineralized tissue regeneration was induced by the transplanted bone representing autogenous bone graft but occurred from the margin of the existing bone.

**Key words:** bone, transplant, *tdTomato*, regeneration, cell kinetics

## INTRODUCTION

Dental implants have become an essential treatment method for edentulous patients, and the number of clinical cases employing dental implants have been increasing all over the world at least past 10 years<sup>1-3</sup>. However, implant therapy is not applicable for all the patients due to insufficient bone mass or an individual's general condition. To induce or regenerate newly formed bone

in an area with defective or lost bone tissue, various bone augmentation techniques have been applied. Various types of bone substitutes have been developed to support bone augmentation; however, the autogenous bone graft is still regarded as the gold standard. Autogenous bone is the only graft material that has osteogenic properties and fulfills all three components of the regeneration triangle (cells, scaffolds,

and growth factors). Although autogenous bone grafts have several obvious disadvantages including post-operative morbidity and limited harvest sites, autogenous bone is believed to be more advantageous than other graft materials, such as allograft, xenografts, and alloplasts, because there is no risk of disease transmission, a short replacement time by newly formed bone, and a lower material cost <sup>4</sup>.

Unfortunately, the healing mechanism of autogenous bone grafts is not well known. Several reports indicate that autogenous bone contains osteogenic cells, which are osteoblasts, osteoclasts, and osteocytes, and those cells could migrate and make bone bridge between original bone and grafted bone <sup>5</sup>. Another report describes osteoblastic cells leaving a bone piece and those cells proliferated and expressed osteoblastic phenotypes in organ cultures <sup>6</sup>. Nyan *et al.* also reported in situ bone regeneration therapy in which osteoconductive scaffolds combined with bioactive molecules might stimulate the local host cells to upregulate osteoblastic differentiation and subsequent bone formation <sup>7</sup>.

Although many studies have been conducted to determine the healing mechanism of autogenous bone grafts, cellular or molecular mechanisms of multiple types of cells behaving around grafted bone remains unclear. Specifically, there are no reports describing which cell growing at the bone contact surface are derived from existing bone or grafted bone. In this study, we investigated the healing mechanisms surrounding grafted bone, at the cellular and molecular levels, employing tissue derived from transgenic mice expressing the red fluorescent protein *in vivo* that make possible to monitor the cellular kinetics *in situ*. To our knowledge, this is the first report demonstrating the cellular dynamics of grafted bone replaced with bone resorption, rather than growth with cell proliferation.

## MATERIALS AND METHODS

### 1. Laboratory animals

This study was approved by the Animal Studies Committee at Iwate Medical University (nos. 27-005; Center for In Vivo Science, Iwate Medical University, Yahaba, Iwate, Japan). Seventeen male nude mice (8 weeks old; BALB/cAJcl-nu/nu: CLEA Japan Inc., Tokyo, Japan) were used in this study (average weight 26.7 g). Twelve male heterozygote Tandem dimer Tomato (tdTomato mice) were also used. Mice overexpressing modified DsRed fluorescent protein were generated using the PITT method are termed tdTomato mice<sup>8</sup>. (Table 1) Animals were maintained at the Iwate Medical University Center for In Vivo Science under appropriate conditions (23°C; 12-h light/dark cycle; humidity 60 ± 10%) with free access to food (Oriental Yeast Co., Ltd., Tokyo, Japan) and water.

**Table 1** Number of mice in each experimental group

	Nude	tdTomato
Experiment 1 CTRL	5	-
Experiment 1 graft group	5	5
Experiment 2	7	7
Total	17	12

### 2. Bone transplant procedures

Calvarial bone derived from tdTomato mice was transplanted into nude mice using the following procedure. Animals were maintained in general anesthesia with oxygen 5.0 L/min and isoflurane (Forlen<sup>®</sup>, DS Pharma Animal Health Co., Ltd., Osaka, Japan) 2.5%. Local anesthesia with 2% lidocaine containing 0.0225 mg adrenaline (Dentsply Sirona Inc., Tokyo, Japan) was used. An incision was made at the top of the head. Scalp, subcutaneous soft tissue, and periosteum were reflected to expose the parietal bones. Bone defects with 4-mm diameters were created at the parietal

bones of 10 nude mice with a 4-mm diameter trephine bur. Simultaneously, five tdTomato mice were sacrificed using carbon dioxide. After the dorsal aspect of the cranium was shaved, parietal bones from tdTomato mice were harvested using the 4-mm diameter trephine bur and transplanted into the calvarial bone defects (Experiment 1). One another transplantation was performed. Four-mm diameter bone plates were harvested from seven tdTomato mice in the same method as described above, and transplanted on the center of calvariae of seven nude mice (Experiment 2). Postoperatively, the periosteum was carefully repositioned and sutured with 5-0 nylon strings (Softretch, GC Tokyo, Japan).

### **3. Radiological analyses**

X-ray micro focus CT scans for nude mice calvarial defects and transplanted calvaria tissue derived from tdTomato mice were performed under general anesthesia with oxygen at 5.0 L / min and isoflurane (Forlen<sup>®</sup>, DS Pharma Animal Health Co., Ltd.) 2.5% at 2, 4, 6, 8, and 20 weeks after surgery. X-ray micro focus CT scans were performed at 24 weeks after surgery on sacrificed animals (Experiment 1). The same scans were performed for nude mice calvariae with onlay grafted cranium tissue derived from tdTomato mice at 2, 4, 6, and 8 weeks after surgery. The same X-ray micro focus CT was performed at 16 weeks on sacrificed mice (Experiment 2). Three-dimensional X-ray images were reconstituted from Vextus Factor compiled storage file (VFF) data obtained from the CT scans, using a micro-CT scanner (eXplore Locus; GE Healthcare Bio-Sciences, Inc., Tokyo, Japan) and three-dimensional analysis software (MicroView Version 2.2, GE Healthcare Bio-Science Inc., Tokyo, Japan).

### **4. Fluorescence imaging**

Fluorescence imaging was performed just prior to X-ray micro focus CT scanning. Living transplanted tdTomato cranium tissues were detected by their red color using a fluorescence image evaluation system (IVIS<sup>®</sup> Lumina Imaging System, PerkinElmer Inc., Waltham, USA). Subsequent image analysis was conducted to quantify the area of red fluorescence, indicating vital tissue, with a computer-based image analyzing software (Image J, NIH). The results are described in relative values to the area of the original tdTomato bone grafts before transplantation (4 mm diameter circle). Data were analyzed by Dunnett's post hoc tests.

### **5. Histological Observation**

At 8 and 16 weeks after onlay bone grafting on the calvariae of nude mice or at 24 weeks after bone grafting on calvaria bone defects, animals were sacrificed by CO<sub>2</sub> asphyxiation. The calvariae were harvested and undecalcified, fresh-frozen samples were sectioned employing Kawamoto's film method<sup>9</sup>. Immunostainings for osteoblast differentiation markers were performed as previously described<sup>10</sup>. Briefly, after adding blocking serum, specimens were incubated with primary antibodies [Mouse Osteopontin/OPN Antibody R&D Systems, Anti-Osteocalcin Antibody (C-Terminus) LS-C42094, LSBio] at room temperature for three hours. After washing with PBS, specimens were incubated with a secondary antibody, Alexa Fluor 488 (Thermo Fisher SCIENTIFIC, Yokohama, Japan). Specimens were observed using a BX51 microscope (Olympus, Tokyo, Japan). Control specimens were incubated directly with secondary antibodies in the absence of primary antibodies and processed as described above. No significant positive immunoreactivity was found in the controls.

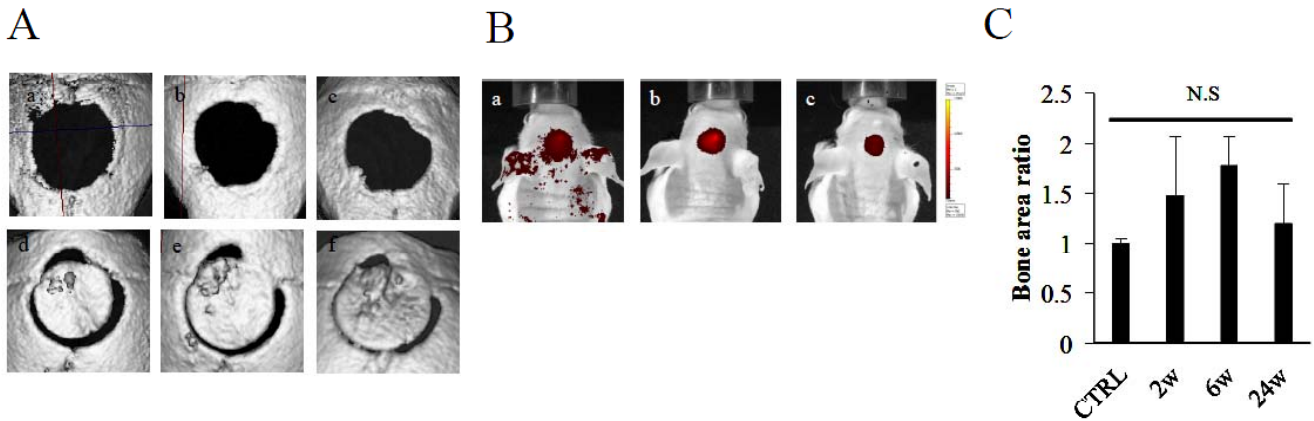


**Figure 1** Micro-CT images of calvarial bone defect (A) (a-2w, b-6w, c-24w) control, (d-2w, e-6w, f-24w) bone grafting. In vivo fluorescence image of calvaria (B) (a-2w, b-6w, c-24w). The fluorescence bone area is quantified (C). Bars and error bars represent means+SE. n = 3 in all groups.

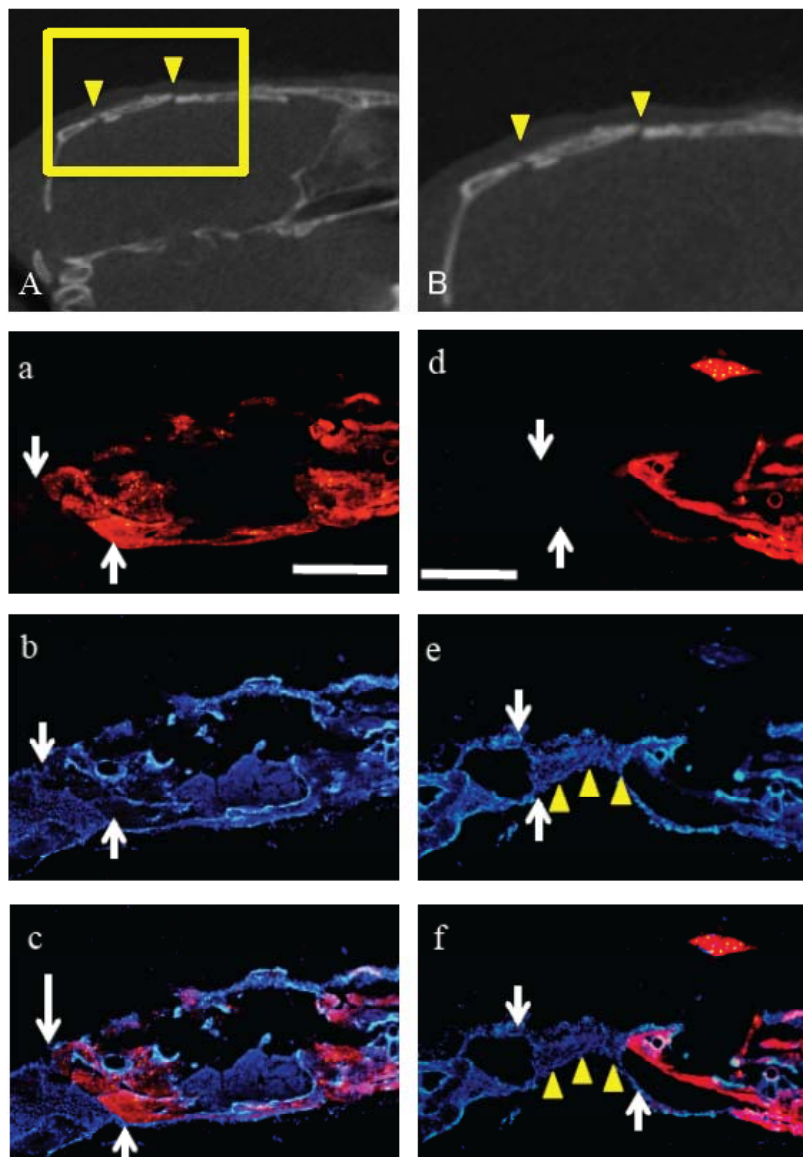


**Figure 2** Micro-CT images of sagittal section of calvarial defect (A) 24 weeks after surgery. Arrow heads represent bone interface with implanted bone. Fluorescent images of bone graft in calvarial defects 24 weeks after transplantation, tdTomato fluorescence (A and D), nucleus stain with DAPI (B and E), and merged images (C and F). Arrows represent the bone boundary and arrow heads represent new bone. Scale bar, 200  $\mu$ m in (A and D).

## RESULTS

### **1. Bone transplant into calvarial bone defect (Experiment 1)**

#### *Radiological observation*

Two weeks after the bone transplantation in the control and experimental groups, the morphology of the bone defect was sharp and rough, but bone regeneration was not observed (Figure 1Aa, Ad). Six weeks after bone grafting in both the control and experimental groups, the marginal morphology of bone defects became rounded (Figure 1Ab, Ae). Little bone regeneration was observed in the control group. The shape of the defect was almost identical to the shape just after the grafting (Figure 1Ab). In the experimental group, there was no obvious bone regeneration at the marginal existing bone in the defect at six weeks. However, at a few points between transplanted bone and existing bone, calcified tissue-like new bone formation was detected (Figure 1Ae). At 24 weeks after bone grafting in the control group, the morphology of the margin in the defect area was considerably more rounded compared than after 2 weeks, but no large change was observed in the diameter of the defect (Figure 1Ac). In contrast, in the experimental group at 24 weeks, the bone defect between transplanted bone and existing bone was filled with newly formed bone at many points (Figure 1Af).

#### **Fluorescence imaging observation**

The red fluorescence was detected by an IVIS<sup>®</sup> Lumina Imaging System (Xenogen Co.) in all transplanted tissue derived from the tdTomato mice. The fluorescence signals showed the maximum value at 6 weeks. The relative intestinal fluorescence signals tended to decrease after 6 weeks, and the fluorescence signals were sustained until 24 weeks. However, there was no significant difference of the area of the red

fluorescence between those time points (Figure 2B, C).

#### **Histological evaluation**

Red fluorescent cells derived from tdTomato mice were observed only in transplanted bone, and no red fluorescent cell infiltration was observed in the existing bone of nude mice (Figure 2c). Between the transplanted and existing bone, tissue regeneration showing no red signal was observed (Figure 2f).

### **2. Onlay transplantation to calvaria bone (Experiment 2)**

Experiment 1 revealed that bony tissue regeneration occurred from the contact margin of transplanted and existing bone, in which newly formed tissue dynamically remodeled. To analyze this in further detail, onlay grafting was carried out to increase the contact area.

#### **Radiological observation**

Two weeks after surgery, the morphology of the transplanted bone margin was sharp and the bone boundary was clear (Figure 3Aa). Four weeks after the surgery, the marginal morphology of the transplanted bone became rounded. Bone-to-bone contact seemed to be established with remodeling (Figure 3Ab). Sixteen weeks after surgery, the transplanted bone margin was considerably more rounded compared to the shape at two weeks, and an area of new, bone-like tissue was formed (Figure 3Ac).

#### **Fluorescence imaging observation**

The red fluorescence was observed in all transplanted bones until 16 weeks after transplantation, while the fluorescence signals were significantly weaker at 16 weeks (Figure 3B, C).

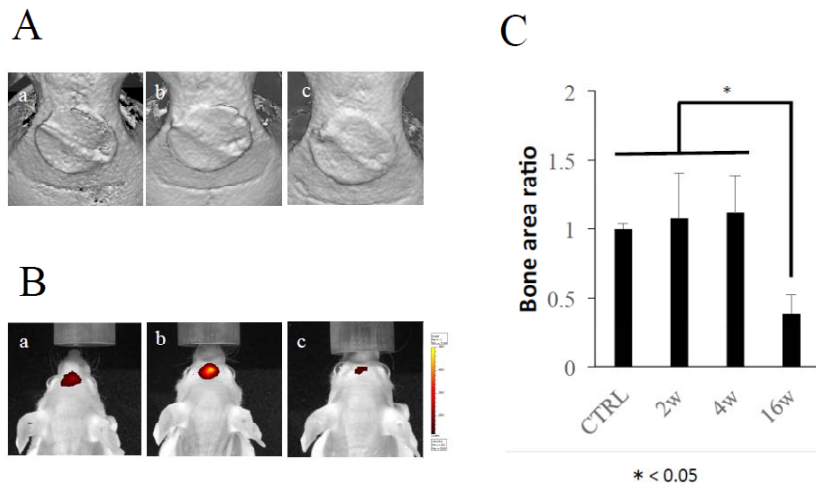


**Figure 3** Micro-CT images of bone on the center of calvariae at (A) (a-2w, b-4w, c-16w) bone grafting. In vivo fluorescence image of calvariae at B is representing of (a-2w, b-4w, c-16w). The fluorescence bone area was measured (C). Bars and error bars represent means and SE, respectively. n = 3 in all groups. (P < 0.05)

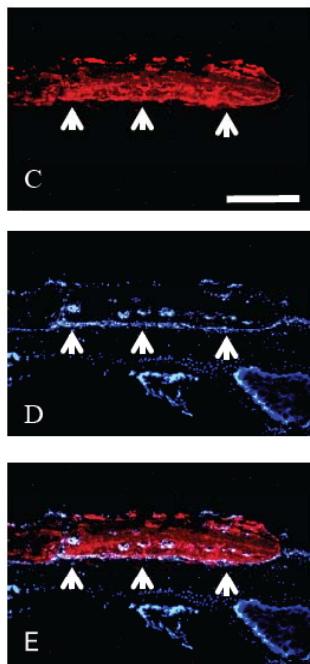
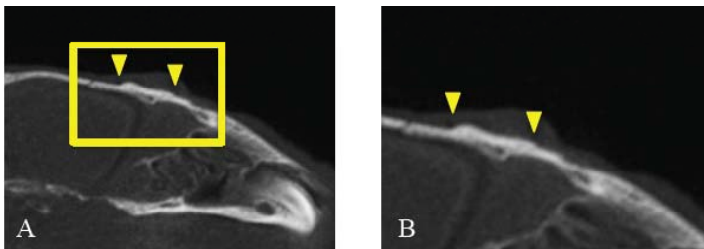


**Figure 4** Micro-CT images of bone on the center of calvariae (A) and (B). Sagittal sections of the implanted bones 16 weeks after surgery. Arrow heads represent bone interface with implanted bone. Fluorescent images of bone graft on calvarial bones 16 weeks after transplantation, tdTomato fluorescence (C), nucleus stain with DAPI (D), and merged image (E). Arrows represent the bone boundary. Scale bar, 500  $\mu$ m in (C).

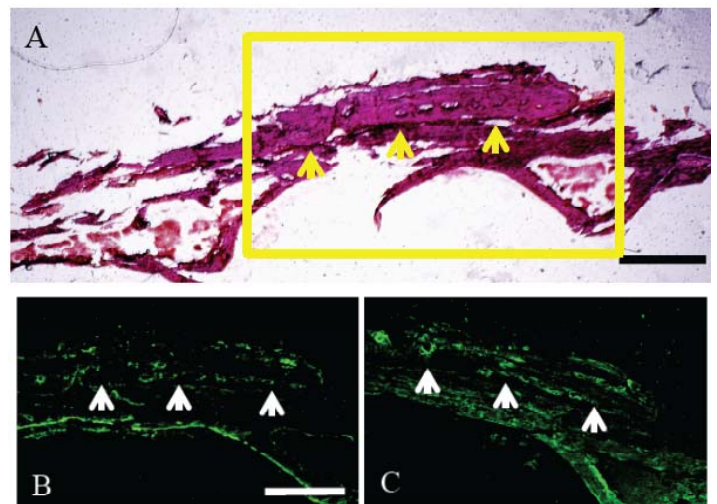


**Figure 5** A is an image of hematoxylin/eosin staining. Expression of osteopontin (B) and osteocalcin (C) at the transplantation site. Arrows represent the bone boundary. Scale bar, 1000  $\mu$ m in A and 500  $\mu$ m in B.

### **Histological evaluation**

Cells showing red fluorescent reaction indicated transplanted cells, and these did not spread into areas of existing bone (Figure 4C). The blue color indicated the area of both existing cells and transplanted cells (Figure 4D). Cells showing both blue and red colors were cells derived from transplanted bone while cells showing blue color only were original existing bone (Figure 4E). Strong expression of osteopontin (OPN) and osteocalcin (OC) was detected in the cortical area of both transplanted and existing bone. (Figure 5B, 5C)

### **DISCUSSION**

Recently, live imaging strategies using fluorescent proteins, such as GFP or DS Red, have been employed to monitor cells and molecular kinetics<sup>11-14</sup>. tdTomato provides a useful alternative to enhanced green fluorescent protein (eGFP) for performing simultaneous detection of fluorescent proteins in histological sections together with fluorescence immunohistochemistry<sup>15</sup>. Thus, tdTomato is a useful tool for tracking cellular or molecular kinetics in medical and pharmaceutical research<sup>16</sup>. However, tdTomato has not yet been employed for cell kinetic analysis in hard tissue research.

Dental implant therapy has become an essential treatment method for edentulous patients, and bone augmentation techniques including autogenous bone grafting are frequently applied to place the dental on severely atrophic jaw bones. Autogenous bone graft is regarded as the gold standard and there are many reports of histological observations surrounding grafted autogenous bones and bone substitutes<sup>4</sup>. However, detailed cell kinetics surrounding the transplanted bones or bone substitutes has not been reported. In this study, the hyper red fluorescent

expression of cells of tdTomato mice was used to follow the movement of cells derived from transplanted bone, and cellular kinetics was demonstrated.

IVIS<sup>®</sup> Lumina Imaging for nude mice calvaria bone defects (Experiment 1) showed that transplanted bone derived from tdTomato mice emitted intense red fluorescent signals for 24 weeks. Those results suggested that transplanted calvaria tissue can be alive for 24 weeks. In the case of onlay grafting (Experiment 2), transplanted bone derived from tdTomato mice emitted intense red fluorescent signals for four weeks and then those fluorescent signals gradually became weaker, suggesting phagocytosis and replacement by cells derived from existing tissue, resulting in the decrease in red fluorescence emittance.

Red fluorescent cells derived from tdTomato mice were detected only in transplanted bone, and no red fluorescent cell infiltration to the existing bone of nude mice was observed in either in Experiment 1 or 2. In contrast, clear existing cell infiltration into transplanted bone was observed in Experiment 1. Those results suggested that transplanted bone might not have osteogenic abilities, even though autogenous bone graft has been regarded as the gold standard<sup>17,18</sup>. Moreover, during tissue regeneration, no red fluorescent signals were detected in the initially empty space between the transplanted bone and the existing bone, indicating that newly formed bone-like tissue was regenerated from the existing bone, but not transplanted bone. Consequently, autogenous bone might not have osteogenic abilities either, which was demonstrated by the transplanted calvaria in this study.

In contrast, no bone regeneration was confirmed in the control group in which calvaria transplantation was not carried out. This fact confirmed that the



transplanted bone was required to induce calcified tissue regeneration. Both OPN and OC expression were detected in transplanted bone. OPN is an early marker for osteoblast differentiation and OC is a terminal differentiation marker that expressed by mature osteoblasts<sup>19-22</sup>. Thus, autogenous bone, represented by transplanted tdTomato calvaria, could provide proper remodeling circumstances, induce bone related regenerative cells, and could be replaced by cells derived from existing bone.

### CONCLUSION

Positive red fluorescent signals and the expression of OPN and OC in transplanted bone after 24 weeks indicated that cells derived from transplants were alive and remodeled by themselves. Moreover, immunohistochemical observation of frozen undecalcified sections demonstrated that cells in the transplant could be replaced by cells derived from existing bone, suggesting that mineralized tissue regeneration was induced by the transplanted bone representing autogenous bone graft and occurred from the margin of the existing bone.

### ACKNOWLEDGMENTS

We would like to thank Drs. Naoyuki Chosa and Seiko Kyakumoto for their helpful advice. This work was supported by JSPS KAKENHI Grant Numbers JP23592864 and JP26462932.

### REFERENCES

- 1) Adell R, Eriksson B, Lekholm U, Brånemark PI, Jemt T. Long-term follow-up study of osseointegrated implants in the treatment of totally edentulous jaws. *Int J Oral Maxillofac Implants* 1990; 5: 347-359.
- 2) Buser D, Mericske-Stern R, Bernard JP, Behneke A, Behneke N, Hirt HP, Belser UC, Lang NP. Long-term evaluation of non-submerged ITI implants. Part 1: 8-year life table analysis of a prospective multi-center study with 2359 implants. *Clin Oral Implants Res* 1997; 8: 161-172.
- 3) Brånemark PI, Svensson B, van Steenberghe D. Ten-year survival rates of fixed prostheses on four or six implants ad modum Brånemark in full edentulism. *Clin Oral Implants Res* 1995; 6: 227-231.
- 4) Nasr HF, Aichelmann-Reidy ME, Yukna RA. Bone and bone substitutes. *Periodontol* 2000 1999; 19: 74-86.
- 5) Fillingham Y, Jacobs J. Bone grafts and their substitutes. *Bone Joint J*, 2016 Jan; 98-B (1 Suppl A):6-9. doi: 10.1302/0301-620X.98B.36350.
- 6) Karsenty G, Wagner EF. Reaching a genetic and molecular understanding of skeletal development. *Dev Cell* 2002; 2: 389-406.
- 7) Nyan M1, Miyahara T, Noritake K, Hao J, Rodriguez R, Kuroda S, Kasugai S. Molecular and tissue responses in the healing of rat calvarial defects after local application of simvastatin combined with alpha tri calcium phosphate. *J Biomed Mater Res B Appl Biomater* 2010; 93: 65-73.
- 8) Ohtsuka M, Ogiwara S, Miura H, Mizutani A, Warita T, Sato M, Imai K, Hozumi K, Sato T, Tanaka M, Kimura M, Inoko H. Pronuclear injection-based mouse targeted transgenesis for reproducible and highly efficient transgene expression. *Nucleic Acids Res*, 2010 Dec; 38(22):e198. doi: 10.1093/nar/gkq860. Epub 2010 Sep 29.
- 9) Kawamoto T. Use of a new adhesive film for the preparation of multi-purpose fresh-frozen sections from hard tissues, whole-animals, insects and plants. *Arch Histol Cytol* 2003; 66: 123-143.
- 10) Otsu K, Kishigami R, Fujiwara N, Ishizeki K, Harada H. Functional role of Rho-kinase in ameloblast differentiation. *J Cell Physiol* 2011; 226: 2527-2534.
- 11) Day RN, Schaufele F. Fluorescent protein tools for studying protein dynamics in living cells: A review. *J Biomed Opt* 2008; 13: 031202. doi: 10.1117/1.2939093.
- 12) Shaner NC, Campbell RE, Steinbach PA, Giepmans BN, Palmer AE, Tsien RY. Improved monomeric red, orange and yellow fluorescent proteins derived from *Discosoma* sp. red fluorescent protein. *Nat Biotechnol* 2004; 22: 1567-1572.
- 13) Bu L, Shen B, Cheng Z. Fluorescent imaging of cancerous tissues for targeted surgery. *Adv Drug Deliv Rev*,



- 2014 Sep 30; 0:21-38. Published online 2014 Jul 24. doi: 10.1016/j.addr.2014.07.008
- 14) Xenopoulos P, Nowotschin S, Hadjantonakis AK. Live imaging fluorescent proteins in early mouse embryos. *Methods Enzymol* 2012; 506: 361-389.
  - 15) Morris LM, Klanke CA, Lang SA, Lim FY, Crombleholme TM. TdTomato and EGFP identification in histological sections: insight and alternatives. *Biotech Histochem* 2010; 85: 379-387.
  - 16) Isherwood B, Timpson P, McGhee EJ, Anderson KI, Canel M, Serrels A, Brunton VG, Carragher NO. Live Cell in Vitro and in Vivo Imaging Applications: Accelerating Drug Discovery. *Pharmaceutics* 2011; 3: 141-170.
  - 17) Danesh-Sani SA, Engebretson SP, Janal MN. Histomorphometric results of different grafting materials and effect of healingtime on bone maturation after sinus floor augmentation: a systematic review and meta-analysis. *J Periodontal Res* 2016; doi: 10.1111/jre.12402. Epub ahead of print.
  - 18) Bertolai R, Catelani C, Aversa A, Rossi A, Giannini D, Bani D. Bone graft and mesenchymal stem cells: clinical observations and histological analysis. *Clin Cases Miner Bone Metab* 2015; 12: 183-187.
  - 19) Denhardt DT, Noda M. Osteopontin expression and function: role in bone remodeling. *J Cell Biochem* 1998; 72: 92-102.
  - 20) Reinholt FP, Hultenby K, Oldberg A, Heinegard D. Osteopontin-a possible anchor of osteoclast to bone. *Proc Natl Acad Sci USA* 1990; 87:4473-4475.
  - 21) Sodek J, Ganss B, McKee MD. Osteopontin. *Crit Rev Oral Biol Med* 2000; 11: 279-303.
  - 22) Standal T, Borset M, Sundan A. Role of osteopontin in adhesion, migration, cell survival and bone remodeling. *Exp Oncol* 2004; 26: 179-184.

(Received, December 1, 2016/  
Accepted, December 16, 2016)

**Corresponding author:**

Hisamoto Kondo, D.D.S.,Ph.,D.  
Department of Prosthodontics and Oral  
Implantology, School of Dentistry  
Iwate Medical University  
19-1 Uchimarui, Morioka 020-8505, Japan  
TEL: +81-019-651-5111  
E-mail: hkondo@iwate-med.ac.jp